Controlling a discrete soliton by a weak beam in waveguide arrays

Truong Xuan Tran and Quang Nguyen-The

Compiled July 11, 2016

Abstract - We investigate numerically and analytically the routing of a moderately confined discrete soliton by using a weak oblique control beam in nonlinear waveguide arrays. Our simulations show that a weak control beam can efficiently route a discrete soliton even when the input power of the weak control beam is less than 20% of the discrete soliton input power. The physical insight into the dragging of the discrete soliton toward the control beam is provided for the first time. The influence of several important parameters such as the initial phase of the weak control beam, peak amplitudes of discrete soliton and control beam, control beam width is investigated in detail.

Index terms - waveguide arrays, discrete soliton, nonlinear fiber optics, optical switches, nonlinear optical devices. © 2016 Optical Society of America

1. INTRODUCTION

Waveguide arrays (WAs) present a unique discrete periodic system to investigate many interesting photonic phenomena such as discrete diffraction [1, 2], discrete solitons (DSs) [1, 3–5], diffractive resonant radiation [6], and supercontinuuum generation in both frequency and wavenumber domains [7]. Recently, WAs have been exploited to simulate fundamental effects in nonrelativistic quantum mechanics such as photonic Bloch oscillations [1, 8–11], and Zener tunneling [12]. Binary WAs have also been intensively used to mimic relativistic phenomena typical of quantum field theory, such as *Zitterbewegung* [13], Klein paradox [14], fermion pair production [15], the Dirac equation in the linear regime [16], and Dirac solitons in the nonlinear regime [17–19].

In applications, WAs may be useful for designing signal-processing circuits, in particular optical switches. One of first works on optical switching in WAs dates back to 1994 [20] where the propagation of a moderately confined discrete soliton (MCDS) extending over five waveguides (and thus, its intensity is also moderate) in the transverse direction was exploited. As shown in Ref. [20], simply by controlling the initial phase difference between excited waveguides it is possible to change the propagation angle of the whole soliton envelope and reach every desirable output channel. Two other poten-

tial schemes of controllable and steerable soliton-based optical switching in nonlinear WAs are discussed for a MCDS (also extending over five waveguides) in Ref. [21]. For the first scheme in Ref. [21] it is suggested that unstable soliton modes (soliton center is localized between two neighboring waveguides) be used to achieve easily steerable propagation of DSs. This is to avoid mode trapping by the effective Peierls - Nabarro potential, which always appears because of the system discreteness. The other scheme proposed in Ref. [21] is based on control of a MCDS with the help of a linear guided wave (or defect mode) that can be excited in an inhomogeneous array. Another interesting scheme to navigate a MCDS on predefined tracks (even with sharp bends) in two-dimensional WAs via interaction with a strongly confined discrete soliton (also referred to as a blocker which is intense and localized practically in just one waveguide) is proposed in Ref. [22]. In the case of incoherent interaction the blockers can block and route MCDSs in 2D networks, thus AND and NOT logic functions can be realized, whereas in the case of coherent interaction the time gating function can be achieved [22].

It is clear that in the regime of operation with MCDSs as shown in Refs. [20–22], the discrete nature of WAs is suppressed and the WA behaves as a bulk medium in some aspects. As a result, MCDSs can propagate almost unhindered and emerge in a predictable region of the array. On the contrary, it is difficult to transversely steer a blocker because it is trapped almost in a single waveguide during propagation due to the Peierls - Nabarro potential in WAs. However, a blocker still can be shifted by a few waveguides in discrete steps via interaction with a low-intensity, wide, tilted beam as shown numerically in Ref. [23] and experimentally in Refs. [24, 25]. The interaction between two DSs under normal incidence with an initial phase difference can also lead to the shift of DSs during propagation as investigated analytically and numerically in Ref. [26], also numerically and experimentally in Ref. [27]. Another approach to steer DSs in WAs is proposed in Ref. [28] just by the longitudinal modulation of the nonlinearity in WAs.

In this paper we propose a new scheme to route a MCDS via interaction with a weak control beam (CB)

Truong X. Tran was with the Max Planck Institute for the Science of Light, Erlangen, Germany. He is now with the Le Quy Don Technical University, Ha Noi, Viet Nam (e-mail: tranxtr@gmail.com).

Quang Nguyen-The was with the University of Electro-Communications, Tokyo, Japan. He is now with the Le Quy Don Technical University, Ha Noi, Viet Nam (e-mail: quanguec@gmail.com).

in WAs. In this scheme the MCDS is launched normally into WAs, whereas the weak CB is launched obliquely into WAs. As shown later in this paper, after the collision the MCDS will be strongly bent toward the CB. The transverse velocity of the MCDS can be efficiently controlled by several parameters such as the initial phase of the weak CB, the peak amplitudes of the weak CB and the MCDS, and the width of the weak CB.

The paper is organized as follows. In Section 2, we provide the physical insight into the steering mechanism of the MCDS after the collision with the weak CB. The influence of the initial phase of the weak CB is also investigated. In Section 3, we study the influence of the initial peak amplitudes of the CB and the MCDS, and also the CB width on the steering of the MCDS. In Section 4, we summarize our results and finish with concluding remarks.

2. THE THEORETICAL MODEL AND INFLUENCE OF THE INPUT CENTRAL WAVE NUMBER OF THE CONTROL BEAM

Light propagation in a discrete, periodic array of Kerr nonlinear waveguides can be described, in the CW regime, by the following well-known dimensionless set of ordinary differential equations [4,5,11]:

$$i\frac{da_n(z)}{dz} + c[a_{n+1}(z) + a_{n-1}(z)] + |a_n(z)|^2 a_n(z) = 0, \quad (1)$$

where a_n is the electric field amplitude in the nth waveguide, z is the dimensionless longitudinal spatial coordinate with the scale $z_0 = 1/(\gamma P_0)$, $c \equiv C/(\gamma P_0)$ is the dimensionless normalized coupling coefficient resulting from the field overlap between neighboring waveguides with C being the physical coupling coefficient in units of $1/m$, γ being the nonlinear coefficient of a single waveguide in units of W^{-1}/m, and P_0 being the power scale in units of W. Equations (1) have two conserved quantities which are the total power P and the Hamiltonian H [11,20]:

$$P = \sum_n |a_n|^2, \quad (2)$$

$$H = -\sum_n [c(a_n^* a_{n+1} + a_n a_{n+1}^*) + 0.5|a_n|^4]. \quad (3)$$

Note that due to the discreteness of the system the equation for momentum conservation does not exist. We will come back to this curious point later.

For the new scheme proposed in this paper we will launch a MCDS normally into the WA, whereas a weak CB is initially tilted. Thus, the initial condition for numerically integrating Eq. (1) is following:

$$a_n(z = 0) = A_{ds}\text{sech}\frac{(n+15)A_{ds}}{\sqrt{2c}} +$$
$$A_{cb}\exp\left[-\frac{(n-20)^2}{w^2}\right]\exp[-ik_0(n-20)]\exp(-i\phi), \quad (4)$$

where the first term with sech function in the right-hand side represents the MCDS [6], the second term in the form of a Gaussian beam represents the CB. In Eq. (4) the parameter A_{ds} is the peak amplitude of the input MCDS which is also inversely proportional to the MCDS width, A_{cb} is the peak amplitude of the weak Gaussian CB, k_0 is the central transverse wave number of the input CB which represents the initial phase difference between the electric fields at waveguides where the CB is excited (thus, k_0 is directly related to the refraction angle of the CB in the WA), parameter ϕ represents the initial phase difference between the CB and the MCDS. It is clear from the input condition in the form of Eq. (4) that the centers of the input MCDS and CB are localized at two waveguides with number $n = -15$ and $n = 20$, respectively. The positions of these centers are not essential in our analysis as long as they are far enough from each other. Therefore, in this work we keep these center positions fixed. The $1/e$ width for amplitudes of the initial CB is equal to $2w$ and also kept constant in our analysis.

In this paper, as a practical example we specify the parameters for the WA as follows: the WA is formed by identical conventional step-index fibers with cladding made of fused silica and core made of silica with 1.8% dopant GeO_2. The core radius is 6 μm and the center-to-center spacing between two adjacent cores $d = 21$ μm. Recent advances in femtosecond-laser writing technologies for WAs of fused silica (see [29]) make the above-proposed WA feasible. The wavelength used for calculation is $\lambda = 1.55$ μm. With this specific WA system the nonlinear coefficient is calculated to be $\gamma = 0.95$ W^{-1}/km, the physical coupling coefficient is calculated to be $C = 159$ m^{-1}, the power scale is chosen to be $P_0 = 140$ kW, and the length scale $z_0 = 1/(\gamma P_0) = 0.0075$ m. The evolution of a MCDS and a CB along the z-axis with the input condition in the form of Eq. (4) according to Eq. (1) is shown in Fig. 1(a). The parameters used for Fig. 1(a) are as follows: the input central wave number of the CB $k_0 = -0.75\pi$, the peak amplitude of the input MCDS $A_{ds} = 0.8$, the peak amplitude of the input CB $A_{cb} = 0.2$, the width parameter of the CB $w = \sqrt{80}$, the initial phase difference between the MCDS and the CB $\phi = 0$, the dimensionless coupling coefficient between neighboring waveguides $c = C/(\gamma P_0) = 1.2$, the WA length $L = 100$, the total number of waveguides used in simulation $N = 421$. With this set of parameters the ratio of the CB input power P_{cb} to the MCDS input power P_{ds} is calculated to be 0.181. The portion of input energy localized in one, three, and five central waveguides of the MCDS is 25.8%, 65.8%, and 86.4%, respectively. As clearly seen from Fig. 1(a),
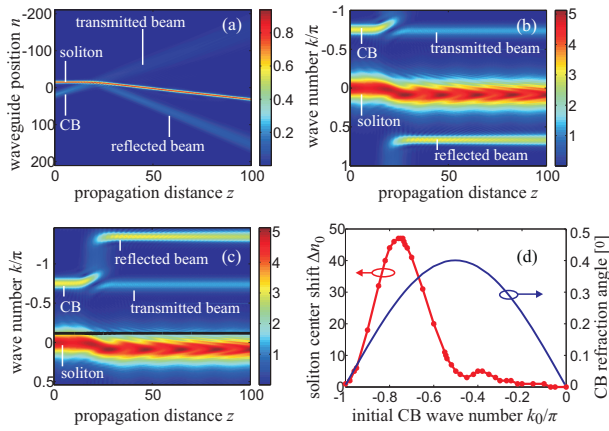
Fig. 1. (Color online) (a,b,c) Propagation of a MCDS and a weak CB in the (n, z) plane (a) and (k, z) plane (b,c). The wave number domain k in (b) is folded within the first Brillouin zone in the interval $[-\pi, \pi]$, whereas the wave number domain k in (c) is within the unfolded interval $[-1.46\pi, 0.54\pi]$. The black solid horizontal line at the level $k = -0.1165\pi$ in (c) represents the evolution of the resulting wave number of all beams. (d) The shift of the MCDS center at the output (red curve with round markers) and the CB refraction angle in the WA (solid blue curve) as functions of the input wave number k_0 of the CB. Parameters: the MCDS peak amplitude $A_{ds} = 0.8$, the CB peak amplitude $A_{cb} = 0.2$, the width parameter of the CB $w = \sqrt{80}$, the initial phase difference between the MCDS and the CB $\phi = 0$, the coupling coefficient $c = 1.2$, the WA length $L = 100$. In (a,b,c) the input central wave number of the CB $k_0 = -0.75\pi$, whereas in (d) this parameter is scanned in the interval $[-\pi, 0]$.

the MCDS and CB are launched normally and obliquely into the WA, respectively. After the collision between them, the CB is split into two beams: the transmitted and reflected beams, while the MCDS is bent toward the reflected beam of the CB. The ratio of the output power of the MCDS to its input power is calculated to be 0.9956, i.e., practically all energy of the input MCDS is conserved during the routing process. Note that before and after the collision the structure of the MCDS is quite stable and its trajectory after the collision is a straight line (although oblique). This behavior of the MCDS after the collision is different from that of the "blocker" after the collision with the signal beam, because in the latter case the blocker is just shifted discretely by just a few waveguides during the collision, then it continues to propagate parallel to the z-axis [24]. It is also clear from Fig. 1(a) that the total momentum K of all beams before and after the collision has different values. This is possible because, as mentioned above, there is no conservation law for momentum in this system. The fact that the soliton is dragged toward the CB is universal in this system and is also observed during the interaction between the "blocker" and "signal" as pointed out, for instance, in Refs. [24, 25]. The conservation of momentum is also broken when a soliton is dragged toward the diffractive resonant radiation emitted from the soliton

itself in WAs [6]. This kind of anomalous recoil is due to the discrete nature of WAs which leads to the folding of the first Brillouin zone as explained both qualitatively and quantitatively in Ref. [6] for the case of diffractive resonant radiation emission. However, in the case of interaction between the blocker and signal, to the best of our knowledge, the dragging of the blocker to the signal has not been given any physical explanation. Now it is time for us to have a closer look at this phenomenon.

We first take the Fourier transform $a(n, z) \rightarrow \tilde{a}(k, z)$, then from Fig. 1(a) we will obtain Fig. 1(b) which shows the evolution of the spectrum $\tilde{a}$ in the (k, z) plain where k is the wave number (or spatial frequency). Due to the discrete nature of WAs the wave number k in Fig. 1(b) is naturally emerged within the first Brillouin zone in the interval $[-\pi, \pi]$. Note that at the input the central wave number of the MCDS and the CB must be equal to 0 (normal incidence), and k_0 = -0.75 (oblique incidence), respectively. After the collision, as shown in Fig. 1(a), the transmitted beam of the CB propagates under the same direction as the input CB, thus in the (k, z) plain the central wave number of the transmitted must be also equal to k_0, see Fig. 1(b). The spectrum of the MCDS after collision is slightly shifted to the positive part of k, whereas the spectrum of the reflected beam of the CB is around $k = 0.66\pi$. However, one can see from Fig. 1(b) that the spectrum of the reflected beam occurs in this region is due to the folding effect of the first Brillouin zone. In the unfolded wave number domain $-1.46\pi \leq k \leq 0.54\pi$, as shown in Fig. 1(c), the spectrum of the reflected beam will be around $k = -\pi - (1 - 0.66)\pi = -1.34\pi$. As a result, if the momentum conservation law is held true in Fig. 1(c), after the collision the spectrum of the MCDS must be shifted to the positive part of k, leading to the bend of the MCDS toward the reflected beam of the CB in Fig. 1(a). Apparently, the conservation law for the total momentum K in Fig. 1(a) and 1(b) is broken, but seems to be held true in Fig. 1(c). Indeed, it is the case as shown below. In order to do that, we just need to calculate the evolution of the total resulting momentum K for all beams in Fig. 1(c) during propagation along z-axis. The problem is reduced to the standard technique of calculating the coordinates of the center of mass in mechanics. Thus, the position of the resulting wave number at each value of z is as follows:

$$K(z) = \frac{\int_{-1.46\pi}^{0.54\pi} k|\tilde{a}(k, z)|^2 dk}{\int_{-1.46\pi}^{0.54\pi} |\tilde{a}(k, z)|^2 dk}, \qquad (5)$$

where the denominator and numerator can be interpreted as the mass and the moment, respectively, of one object with uniform density in mechanics which is confined between the curve $|\tilde{a}(k)|^2$ and the k-axis in the interval $-1.46\pi \leq k \leq 0.54\pi$. This resulting wave number for the case in Fig. 1(c) is calculated to be $K \simeq -0.115\pi$ [black solid horizontal line in Fig. 1(c)] and is practically constant during propagation. Unlike Eq. (2) and Eq. (3) which one can always use to calculate the total power P

and Hamiltonian H, one can only use Eq. (5) to calculate the resulting wave number K under the condition that the spectra of all beams before and after the collision do not significantly overlap at the upper and lower limits of the unfolded wave number domain k. We want to emphasize that although the difference of the upper and lower limits of two integrals in Eq. (5) is always equal to 2π, the specific values of these two limits must be found for each individual case. In the case of Fig. 1(b) and 1(c) the criteria for choosing the unfolded wave number are as follows: (i) the spectrum of the reflected beam of the CB is connected to the spectrum of the input CB, (ii) and at the same time the spectrum of the MCDS remains intact. Therefore, the upper limit of the unfolded wave number domain must be located between the spectrum of the MCDS and the spectrum of the reflected beam of the CB in Fig. 1(b), thus this upper limit must be around 0.5π. In Fig. 1(c), as mentioned above, we choose the unfolded wave number domain $k \in$ [-1.46π, 0.54π] and the resulting wave number K is calculated to be around -0.115π. If the unfolded wave number domain is slightly changed such that the two above-mentioned criteria are met, for instance $k \in$ [-1.5π, 0.5π], then K is also calculated to be around -0.115π and conserved during propagation. Note that in the case of Fig. 1 the total number of waveguides $N = 421$, thus the grid for the wave number domain in Fig. 1(b) and 1(c) is very fine with the step being equal to $2\pi/N$ and the wave number domain there can be treated as quasicontinuous. In this case, the integration in Eq. (5) makes sense. However, if N is not large enough, then the grid for the wave number domain can be rough, and in that case one should use the summation instead of the integration in Eq. (5). Note also that the dragging mechanism of the MCDS toward the reflected beam of the CB explained above can be applied for the case of interaction between a blocker and a signal beam.

As shown in Fig. 1(a), because the transmitted and reflected beams of the CB are weak, these linear waves gradually spread in space due to diffraction. Meanwhile, the MCDS, as a nonlinear localized soliton, propagates under the same direction after collision without any distortion of its shape. If the WA length is much longer than $L = 100$ used in Fig. 1, then our simulations show that these two trends are also observed. Namely, the transmitted and reflected beams of the CB continue to broaden in space during propagation, whereas the MCDS continues to maintain its shape and propagation direction. As a result, for longer WA length the main features of Fig. 1(b) after collision remain unchanged.

At the output in Fig. 1(a) the center of the MCDS is shifted by $\Delta n_0 = 47$ waveguides as compared to the center of the input MCDS. In what follows we show that the shift of the MCDS center can be efficiently controlled by different ways. In Fig. 1(d) we plot the MCDS center shift Δn_0 (red curve with round markers) and the CB refraction angle α in the WA in units of degrees (solid blue curve) as functions of the central input wave num-

ber k_0 of the CB in the interval $-\pi \leq k_0 \leq 0$ (half a period). Except for the change in k_0, all other parameters in Fig. 1(d) are the same as in Fig. 1(a). The CB refraction angle in the WA before the collision with the MCDS is the propagation angle of the CB formed by the CB with the z-axis, and can be defined as $\alpha =$ atan$[(d/z_0)v]$, where $v = $ -2$c$sin(k_0) is the transverse velocity of the CB in the WA (see Ref. [11], pages 12-13). As clearly shown in Fig. 1(d) when k_0 is within the interval $-0.5\pi \leq k_0 \leq 0$ the routing of the MCDS is not efficient, because the center of the MCDS can be shifted only by less than 6 waveguides. However, the MCDS center shift Δn_0 quickly rises when k_0 gradually decreases in the interval $-0.75\pi \leq k_0 \leq -0.5\pi$, reaching the maximum shift $\Delta n_0 = 47$ when $k_0 = -0.75\pi$. If k_0 decreases further down to $-\pi$, the MCDS center shift quickly decreases from 47 waveguides down to 0 waveguides. This is due to the fact that the CB refraction angle in the WA will decrease to zero when k_0 decreases from -0.75π down to $-\pi$, leading to the decrease in interaction between the CB and MCDS. In the interval $-2\pi \leq k_0 \leq -\pi$ the CB propagates in the downward direction from the very beginning, thus it cannot collide with the MCDS. Note that with the input central wave number $k_0 = -0.5\pi$ the CB will undergo the diffraction-less propagating [11]. This value of $k_0 = -0.5\pi$ is used in Refs. [24, 25] to discretely shift the intense blocker. However, in our work, using this value of $k_0 = -0.5\pi$ for the CB will be inefficient in routing the MCDS.

3. INFLUENCE OF THE BEAMS PEAK AMPLITUDES AND THE CONTROL BEAM WIDTH

In this Section we investigate the influence of several important parameters on the routing of the MCDS. First, we want to investigate the role of the peak amplitude A_{cb} of the input CB. Figure 2(a) shows the propagation of a MCDS and a CB. All parameters used in Fig. 2(a) are exactly the same as in Fig. 1(a) with the only exception that the input peak amplitude of the CB $A_{cb} = 0.32$ in Fig. 2(a) instead of $A_{cb} = 0.2$ in Fig. 1(a). Thus, the CB input power in Fig. 2(a) is 2.56 times larger than that value in Fig. 1(a), and the ratio of input powers $P_{cb}/P_{ds} = 0.4634$ now in Fig. 2(a) instead of the ratio value 0.181 in Fig. 1(a). As a result, the more intense CB in Fig. 2(a) is capable of routing the MCDS by $\Delta n_0 = 86$ waveguides at the output as compared to just 47 waveguides in Fig. 1(a).

In Fig. 2(b) we plot the dependence of the MCDS center shift Δn_0 at the output (red curve with round markers) and the ratio of the CB input power to the MCDS input power (solid blue curve) as functions of the peak amplitude A_{cb} of the CB. As clearly shown in Fig. 2(b), when A_{cb} is still small ($A_{cb} < 0.35$, which means the CB is also still weak as compared to MCDS: $P_{cb}/P_{ds} < 0.55$) the MCDS center shift Δn_0 quickly rises with the increase in A_{cb}. However, the saturation for Δn_0 is ob-
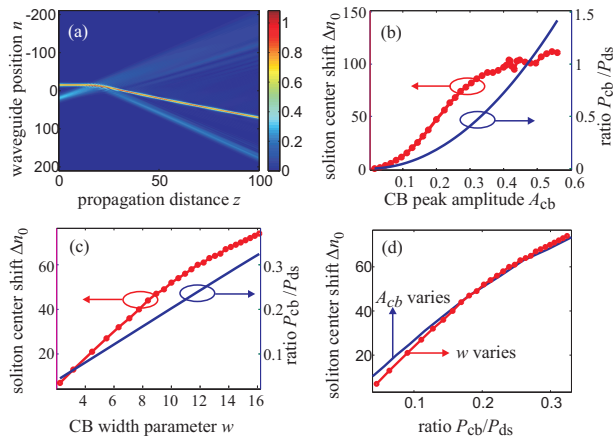
Fig. 2. (Color online) (a) Propagation of a MCDS and a CB when the CB peak amplitude $A_{cb} = 0.32$ (the CB width parameter is fixed at the value $w = \sqrt{80}$). (b) Dependence of the MCDS center shift (red curve with round markers) and the input power ratio P_{cb}/P_{ds} (solid blue curve) as functions of the CB peak amplitude A_{cb}. (c) Dependence of the MCDS center shift (red curve with round markers) and the input power ratio P_{cb}/P_{ds} (solid blue curve) as functions of the CB width parameter w (the CB peak amplitude is fixed at the value $A_{cb} = 0.2$). (d) Dependence of the MCDS center shift as a function of the input power ratio P_{cb}/P_{ds} for two cases: blue solid curve - when A_{cb} varies and w is fixed; red curve with round markers - when w varies and A_{cb} is fixed. Except for changes in A_{cb} and w, all other parameters are the same as in Fig. 1(a).

served if A_{cb} is increased further. This is understandable, because our simulations (not shown here) reveal that when the peak amplitude A_{cb} of the input CB is too large (while keeping the CB width constant), the CB will quickly spread out even before the collision with the MCDS. Thus, the interaction between the MCDS and the CB is not very efficient.

We now investigate the influence of the CB width parameter w on the routing of the MCDS. In Fig. 2(c) we plot the dependence of the MCDS center shift Δn_0 at the output (red curve with round markers) and the input power ratio P_{cb}/P_{ds} (solid blue curve) as functions of the CB width parameter w while fixing $A_{cb} = 0.2$ and all other parameters as in Fig. 1(a). Obviously, in this case, the input power P_{cb} of the CB is a linear function of its width parameter w (blue straight line in Fig. 2(c)). As clearly shown in Fig. 2(c), the MCDS center shift Δn_0 also quickly rises when w is increased.

In Fig. 2(d) we plot the dependence of the MCDS center shift Δn_0 at the output as a function of the input power ratio P_{cb}/P_{ds} for two cases: when w varies, but A_{cb} is fixed to be equal to 0.2 (red curve with round markers); and when A_{cb} varies, but w is fixed to be equal to $\sqrt{80}$ (blue solid curve). All other parameters in Fig. 2(d) are the same as in Fig. 1(a). As clearly shown in Fig. 2(d), even when $P_{cb}/P_{ds} < 0.2$ the weak CB still can efficiently route the MCDS by up to about 50 waveguides

at the output of a WA with length $L = 100$. The MCDS center shift Δn_0 can be even much more significant if the WA length is increased. Figure 2(d) also reveals that if the CB is weak (while the input power of the MCDS is fixed), then the MCDS center shift Δn_0 at the output mainly depends on the input power P_{cb} of the CB in a proportional manner, but only slightly depends on the way how to obtain that value P_{cb} (whether by varying the input amplitude A_{cb} or width parameter w of the CB).
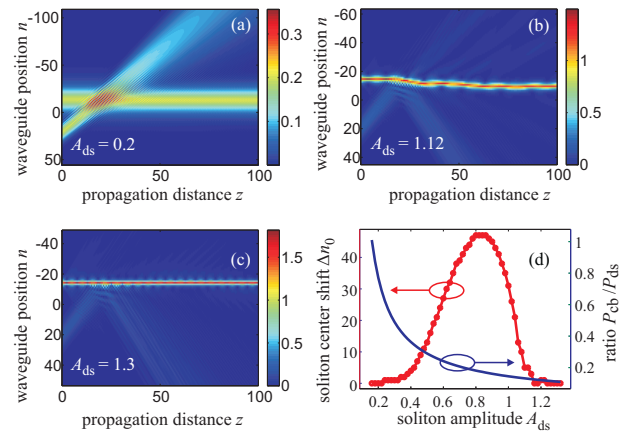
Fig. 3. (Color online) (a,b,c) Propagation of a MCDS and a CB when the MCDS peak amplitude $A_{ds} = 0.2$, 1.12, and 1.3, respectively. (d) Dependence of the MCDS center shift Δn_0 (red curve with round markers) and the input power ratio P_{cb}/P_{ds} (solid blue curve) as functions of the MCDS peak amplitude A_{ds}. Except for changes in A_{ds} all other parameters are the same as in Fig. 1(a).

Now we analyze in detail the influence of the peak amplitude A_{ds} of the input MCDS in its routing process. In Fig. 3(a), (b), and (c) we show the propagation of a MCDS and a CB when the input peak amplitude of the MCDS $A_{ds} = 0.2$, 1.12, and 1.3, respectively, with all other parameters being the same as in Fig. 1(a). In Fig. 3(a) the input peak amplitude of the MCDS is low ($A_{ds} = 0.2$), thus, the MCDS width is large. As a result the CB and MCDS in Fig. 3(a) practically operate in the linear regime and propagate though each other with minimum influence from the other beam. On the contrary, in Fig. 3(b) the input peak amplitude of the MCDS is high ($A_{ds} = 1.12$), which means almost all of energy of the input MCDS is trapped in just a few waveguides. To be more specific, the portion of input energy localized in one, three, and five central waveguides of the MCDS is 36.2%, 80.7%, and 95.2%, respectively. As a result, in Fig. 3(b), due to the combination of the discreteness and strong nonlinearity, the weak CB is only able to shift the MCDS by just a few waveguides during interaction between them. Note that in Fig. 3(b) after the interaction the MCDS practically propagates parallel to the z-axis. This scenario is somewhat similar to the routing of a blocker by a diffractionless signal beam reported in Refs. [24, 25]. If we increase the peak amplitude of the

input MCDS further to the value $A_{ds} = 1.3$ (and thus, its spatial localization is even more enhanced) as in Fig. 3(c), then the weak CB cannot shift the MCDS at all during their collision. In Fig. 3(d) we plot the dependence of the MCDS center shift Δn_0 at the output (red curve with round markers) and the input power ratio P_{cb}/P_{ds} (solid blue curve) as functions of the peak amplitude A_{ds} of the input MCDS while fixing all other parameters as in Fig. 1(a). Because the input power P_{ds} of the MCDS is directly proportional to its peak amplitude A_{ds} at the input, therefore, when the input power P_{cb} of the CB is fixed the ratio P_{cb}/P_{ds} is inversely proportional to A_{ds} as shown by the solid blue curve in Fig. 3(d). The bell shape of the red curve with round markers in Fig. 3(d) is now understandable. When $A_{ds} < 0.4$, two beams practically operate in the linear regime and almost do not change their propagation directions, therefore, the wide and weak DS is shifted by just a few waveguides and Δn_0 is negligible as illustrated in Fig. 3(a). When $A_{ds} > 1.12$, the narrow and intense DS is trapped in several waveguides due to the combination of strong nonlinearity and discreteness, therefore, Δn_0 is also negligible as illustrated in Fig. 3(b) and (c). In the intermediate regime when $0.4 < A_{ds} < 1.12$, the MCDS is strongly routed by the weak CB with Δn_0 reaching its peak if $A_{ds} \simeq 0.8$ as illustrated in Fig. 1(a).

In the rest of this work we discuss the influence of the initial phase difference ϕ between the DS and the CB in Eq. (4) in the routing of the DS. It is well-known that the interaction of two spatial solitons which initially propagate parallel to each other in WAs depends strongly on their initial phase difference [18, 26, 27]. In the case of interaction between a blocker (launched normally into WAs) with an oblique signal beam one can control the shift of the blocker within a range of just few waveguides by varying the initial phase difference between them [23, 24]. Our simulations also confirm that Δn_0 can be varied within a range of just few waveguides by changing the initial phase difference ϕ between a weak CB and an intense DS [when $A_{ds} > 1.1$ as the case in Fig. 3(b)]. The variation of Δn_0 can be even larger up to 10 waveguides if a strong CB (e.g., $A_{cb} = 0.6$) is used to route the MCDS in Fig. 1. However, our simulations reveal that the initial phase difference ϕ practically does not play any significant role in the routing of a MCDS, or a weak DS by *a weak oblique CB*. For instance, in Fig. 1(a) and 3(a) if we change the value of ϕ while fixing all other parameters, then Δn_0 will not be different. It is easy to understand why ϕ does not play any role at all in routing *a weak DS by a weak CB*, because these two beams are in the linear regime and propagate independently of each other [see Fig. 3(a)]. However, the reasons why ϕ has some influence on routing a strong blocker, but does not have any significant role in routing a MCDS by *a weak oblique CB* as shown in Fig. 1(a) are still open to discussion.

4.   SUMMARY

In conclusion, we demonstrate numerically that a weak control beam can efficiently route a moderately confined discrete soliton in waveguide arrays with Kerr nonlinearity even when the ratio of the control beam input power to that of the discrete soliton is less than 20%. The dragging of the discrete soliton toward the control beam is well-known in literatures, but the physical mechanism behind this effect is only provided for the first time in this work, to the best of our knowledge. The initial phase of the CB is an essential parameter in this routing process and it turns out that the optimal value of this initial phase for enhancing the routing should be around -0.75π instead of -0.5π as often used in other works for diffractionless propagation of the CB. When the input power of the CB increases, the center shift of the MCDS at the output also increases and only slightly depends on the way how to reach that input power of the CB.

References

1. D. N. Christodoulides, F. Lederer, and Y. Silberberg, "Discretizing light behaviour in linear and nonlinear waveguide lattices," *Nature*, vol. 424, pp. 817-823, Aug. 2003.
2. A. L. Jones, "Coupling of Optical Fibers and Scattering in Fibers," *J. Opt. Soc. Am.*, vol. 55, pp. 261-271, Mar. 1965.
3. D. N. Christodoulides and R. I. Joseph, "Discrete self-focusing in nonlinear arrays of coupled waveguides," *Opt. Lett.*, vol. 13, pp. 794-796, Sep. 1988.
4. Y. S. Kivshar and G. P. Agrawal, *Optical Solitons: from Fiber to Photonic Crystals*, 5th ed. (Academic, 2003).
5. G. P. Agrawal, *Applications of Nonlinear Fiber Optics*, 2nd. Academic Press, 2008.
6. Tr. X. Tran and F. Biancalana, "Diffractive resonant radiation emitted by spatial solitons in waveguide arrays," *Phys. Rev. Lett.*, vol. 110, pp. 113903-113906, Mar. 2013.
7. Tr. X. Tran, D. C. Duong, and F. Biancalana, "Supercontinuum generation in both frequency and wave number domains in nonlinear waveguide arrays," *Phys. Rev. A*, vol. 89, pp. 013826-013831, Jan. 2014.
8. U. Peschel, T. Pertsch, and F. Lederer, "Optical Bloch oscillations in waveguide arrays," *Opt. Lett.*, vol. 23, pp. 1701-1703, Nov. 1998.
9. T. Pertsch, P. Dannberg, W. Elflein, A. Bräuer, and F. Lederer, "Optical Bloch oscillations in temperature tuned waveguide arrays," *Phys. Rev. Lett.*, vol. 83, pp. 4752-4755, Dec. 1999.
10. G. Lenz, I. Talanina, and C. M. de Sterke, "Bloch oscillations in an array of curved optical waveguides," *Phys. Rev. Lett.*, vol. 83, pp. 963-966, Aug. 1999.

11. F. Lederer, G. I. Stegeman, D. N. Christodoulides, G. Assanto, M. Segev, and Y. Silberberg, "Discrete solitons in optics," *Phys. Reports*, vol. 463, pp. 1-126, Apr. 2008.

12. M. Ghulinyan, C. J. Oton, Z. Gaburro, L. Pavesi, C. Toninelli, and D. S. Wiersma, "Zener Tunneling of Light Waves in an Optical Superlattice," *Phys. Rev. Lett.*, vol. 94, 127401-127404, Apr. 2005.

13. S. Longhi, "Photonic analogue of *Zitterbewegung* in binary waveguide arrays," *Opt. Lett.*, vol. 35, pp. 235-237, Jan. 2010.

14. F. Dreisow, R. Keil, A. Tünnermann, S. Nolte, S. Longhi, and A. Szameit, "Klein tunneling of light in waveguide superlattices," *Europhys. Lett.*, vol. 97, pp. 10008-10013, Jan. 2012.

15. S. Longhi, "Classical simulation of relativistic quantum mechanics in periodic optical structures," *Appl. Phys. B*, vol. 104, pp. 453-468, Jul. 2011.

16. J. M. Zeuner, N. K. Efremidis, R. Keil, F. Dreisow, D. N. Christodoulides, A. Tünnermann, S. Nolte, and A. Szameit, "Optical analogues for massless Dirac particles and conical diffraction in one dimension," *Phys. Rev. Lett.*, vol. 109, pp. 023602-023606, Jul. 2012.

17. Tr. X. Tran, S. Longhi, and F. Biancalana, "Optical analogue of relativistic Dirac solitons in binary waveguide arrays," *Ann. Phys.*, vol. 340, pp. 179-187, Jan. 2014.

18. Tr. X. Tran, X. N. Nguyen, and D. C. Duong, "Dirac soliton stability and interaction in binary waveguide arrays," *J. Opt. Soc. Am. B*, vol. 31, pp. 1132-1136, Apr. 2014.

19. Tr. X. Tran, X. N. Nguyen, and F. Biancalana, "Dirac solitons in square binary wave guide lattices," *Phys. Rev. A*, vol. 91, pp. 023814-023820, Feb. 2015.

20. W. Królikowski, U. Trutschel, M. Cronin-Golomb, and C. Schmidt-Hattenberger, "Solitonlike optical switching in a circular fiber array," *Opt. Lett.*, vol. 19, pp. 320-322, Mar. 1994.

21. W. Królikowski and Y. S. Kivshar, "Soliton-based optical switching in waveguide arrays," *J. Opt. Soc. Am. B*, vol. 13, pp. 876-887, May 1996.

22. D. N. Christodoulides and E. D. Eugenieva, "Blocking and routing discrete solitons in two-dimensional networks of nonlinear waveguide arrays," *Phys. Rev. Lett.*, vol. 87, pp. 233901-233904, Nov. 2001.

23. O. Bang and P. D. Miller, "Exploiting discreteness for switching in waveguide arrays," *Opt. Lett.*, vol. 21, pp. 1105-1107, Aug. 1996.

24. J. Meier, G. I. Stegeman, D. N. Christodoulides, Y. Silberberg, R. Morandotti, H. Yang, G. Salamo, M. Sorel, and J. S. Aitchison, "Beam interactions with a blocker soliton in one-dimensional arrays," *Opt. Lett.*, vol. 30, pp. 1027-1029, May 2005.

25. J. Meier, G. I. Stegeman, D. N. Christodoulides, R. Morandotti, G. Salamo, H. Yang, M. Sorel, Y. Silberberg, and J. S. Aitchison, "Incoherent blocker soliton interactions in Kerr waveguide arrays," *Opt. Lett.*, vol. 30, pp. 3174-3176, Dec. 2005.

26. A. B. Aceves, C. De Angelis, T. Peschel, R. Muaschall, F. Lederer, S. Trillo, and S. Wabnitz, "Discrete self-trapping, soliton interactions, and beam steering in nonlinear waveguide array," *Phys. Rev. E*, vol. 53, pp. 1172-1189, Jan. 1996.

27. J. Meier, G. I. Stegeman, Y. Silberberg, R. Morandotti, and J. S. Aitchison, "Nonlinear Optical Beam Interactions in Waveguide Arrays," *Phys. Rev. Lett.*, vol. 93, pp. 093903-093906, Aug. 2004.

28. G. Assanto, L. A. Cisneros, A. A. Minzoni, B. D. Skuse, N. F. Smyth, and A. L. Worthy, "Soliton Steering by Longitudinal Modulation of the Nonlinearity in Waveguide Arrays," *Phys. Rev. Lett.*, vol. 104, pp. 053903-053906, Feb. 2010.

29. A. Szameit, D. Blömer, J. Burghoff, T. Pertsch, S. Nolte, and A. Tünnermann, "Hexagonal waveguide arrays written with fs-laser pulses," *Appl. Phys. B*, vol. 82, pp. 507-512, Jan. 2006.

Truong X. Tran was born in Thai Binh city, Viet Nam, in 1975. He received the B.S. and M.S. in laser techniques and laser technologies from the St.-Petersburg National Research University of Information Technologies, Mechanics and Optics (in Russia) in 2002 and 2004, and the Ph.D. degree in optics from the same university in 2007. In 2009-2012, he was a postdoctoral researcher at the German Max Planck research group "Nonlinear Photonic Nanostructures" at the Max Planck Institute for the Science of Light, Erlangen, Germany. Since 2013 he has been a lecturer at the Department of Physics, Le Quy Don University in Ha Noi, Viet Nam. He is the author of about 30 scientific articles in peer-reviewed journals. His research interests include linear and nonlinear fiber optics, optical solitons, waveguide arrays, photonic crystal fibers, simulation of quantum effects with optical platforms, and laser technologies.

Dr. Tran has won a project to establish a German Max Planck Partner Group in Ha Noi from 2013 - 2016.

Quang Nguyen-The was born in Bac Ninh, Viet Nam, in 1978. He received B.E. degree from National Defense Academy, Japan in 2004, M.E. degree in 2009 and the Ph.D degree in 2012 from the University of Electro-Communications, Tokyo, Japan. He was as a postdoctoral fellow researcher in Department of Communication Engineering and Informatics, the University of Electro-Communications, Tokyo, Japan from 2012 to 2014. Dr. Quang is a Member of Institute of Electronics, Information and Communication Engineers of Japan. He was the recipient of the Young Scientist Award in the 15th OptoElectronics and Communications Conference (OECC 2010) presented by the IEEE Photonics Society Japan Chapter. His research interest is in all-optical signal processing for WDM and OTDM systems. He is currently a Lecturer of the Le Quy Don Technical University, Ha Noi, Viet Nam.